arXiv:cond-mat/9806347v2 [cond-mat.str-el] 27 Oct 1998

Magnetic Resonance of the Intrinsic Defects of the Spin-Peierls Magnet $CuGeO_3$

A.I.Smirnov, V.N.Glazkov
P.L.Kapitza Institute for physical problems RAS, 117334 Moscow, Russia

L.I.Leonyuk, A.G.Vetkin,
Moscow State University, 119899 Moscow, Russia

R.M.Eremina
E.K.Zavoisky Physical Technical Institute RAS, 420029 Kazan, Russia

The magnetic resonance of the pure monocrystals of $CuGeO_3$ is studied in the frequency range 9-75 GHz and in the temperature interval 1.2-25 K.
The splitting of the ESR line into several spectral components is observed below 5 K, in the temperature range where the magnetic susceptibility is suppressed by the spin-Peierls dimerization. The analysis of the magnetic resonance signals allows one to separate the signals of the S =1/2 and $S = 1$ defects of the spin-Peierls phase. The values of the g-factor, corresponding to these signals are close to the characteristic values of the Cu^{2+}-ion The additional line of the magnetic resonance is characterized by the strong anisotropy of the $g-$factor and by the threshold-like increase of the microwave susceptibility when the microwave power is increasing. This threshold-like increase of the susceptibility is observed both at the resonance value of the magnetic field and at the wings of the resonance line. These signals are supposingly attributed to two types of the planar magnetic defects, arising at the boundaries of the domains of the spin-Peierls state with the different values of the phase of the dimerization.

PACS numbers: 64.70.Kb 75.10.Jm 77.22Ch 75.40.Cx

I. INTRODUCTION

The inorganic compound $CuGeO_3$ possesses the magnetic and crystallographic properties of the spin-Peierls crystals and is intensively studied during the last years by different methods. The magnetic structure of this crystal is based on the 1D-chains of S=1/2 Cu^{2+} ions, elongated along the $c-$ axis of the orthorombic crystal. The drop of the magnetic susceptibility is found below the temperature of the spin-Peierls[1] transition. This drop of the susceptibility is accompanied by the lattice period doubling in the directions a and c[2,3]. The change of the magnetic properties is provided by the formation of dimers of magnetic atoms, being placed closer than in the initial state, with the exchange integral being larger than that in the state above the transition point. The ground state of the spin-Peierls crystal is singlet, and the excited states are separated by an energy gap. The magnetic susceptibility is to be equal to zero at absolute zero. The values of the gap and of the spin-Peierls transition temperature depend on the variation of the exchange integral along the dimerised chain[4,5]. Note that the undimerised chain of the S =1/2 spins with the Heisenberg antiferromagnetic exchange has the gapless spectrum, and the ground state is not the Neel state[6].

The described transition results from the instability produced by the interaction of the 1D spin chains with the 3D elastic lattice of the crystal. Spin chains construct a quasi-one-dimensional antiferromagnet, but the reconstruction of the crystal at the transition is of three dimensional character and the dimers are placed in an ordered sublattice. The displacements of copper ions are directed along the c-axes and the rotations of the oxygen octahedra surrounding the copper ions occur in the ab-plane[2]. The displacements of copper ions of the neighboring chains are opposite-phase-correlated, i.e. the dimers coincide after the translations by vectors $\mathbf{a}+\mathbf{c}$ or $\mathbf{b/2}+\mathbf{c}$. Here $\mathbf{a},\mathbf{b},\mathbf{c}$ are the primitive translations of the undimerized phase. The period of the Cu-sites displacement along the $b-$direction is equal to a half of the period of the lattice in the high-temperature phase, because there are two Cu-ions per primitive cell, separated by the translation $\mathbf{b}/2$. The octahedra rotations are correlated in an analogous way, the octahedra coincide after the translations mentioned. Thus the reconstruction of the lattice is accompanied by the dimerization of copper atoms along the $c-$ axis and of the oxygen atoms along a and b-axes. The displacements δz_{klm} of the Cu^{2+}-ions relative to the undimerised lattice may be described by the relation:

$$\delta z_{klm} = \xi \cos[((k+l+m))\pi + \psi] \qquad (1)$$

Here ξ is the amplitude of the displacement, k, l, m are the coordinates of the Cu-ions respective to some reference ion in the units of$a, b/2, c$ in the system of coordinates attributed to the crystal axes a, b, c. The phase ψ is the phase of dimerization, it can take one of two values: 0 or π following[7]. The state of the crystal is doubly degenerated with respect to this parameter.

The main characteristics of the spin-Peierls state in $CuGeO_3$, are as follows[3]: the temperature of the transition $T_{SP} = 14.2$ K, the intrachain exchange integral J_c is

10.6 meV, the energy gap at absolute zero $\Delta = 2$ meV, the relative variation of the exchange integral in the dimerised chain δ=0.042. The interchain-to-intrachain exchanges ratio are J_b/J_c =0.11, J_a/J_c = -0.011. The maximum displacement of the Cu-ions is 0.007 A^o.

The magnetic susceptibility data and the results of the studies of the crystallographic and magnetic structure and the investigations of the excitation spectra of $CuGeO_3$ agree mainly with the concept of the spin-Peierls transition (see, e.g.[3]).

The freezing out of the magnetic susceptibility of the real samples does not occur for all the 100 per cents. The magnetic susceptibility of the best samples vanishes approximately for 10 times, the susceptibility takes the minimum value at 5 K and demonstrates an increase at the further diminishing of the temperature. The residual susceptibility might be ascribed to the dangling ends of the chains or to the impurities. There are also other suggestions, given below in this paper.

The insertion of the defects in the lattice or the doping of the magnetic subsystem results in the lowering of the spin-Peierls transition temperature, and in the 3D long range antiferromagnetic order at more lower temperatures[8,9]. After the doping by 0.07% Si or by 2%Zn the Neel temperature is 4 K . The remarkable feature of the antiferromagnetic ordering stimulated by the impurities is the coexistence of the Neel and spin-Peierls states. The mean spin-per-site value is of several tenths of the nominal value. The suppression of the dimerization in the vicinity of the defect is the reason for the transformation of the nonmagnetic spin-Peierls state into the antiferromagnetic state[7,10]. The absence of the dimerization leads to the antiferromagnetic correlation of several spins around the defect along the chain and in the perpendicular directions because of the exchange interactions. The average value of the spin projection diminishes with moving away from the defect. The correlated areas of the neighboring defects overlap, providing the long range magnetic order. At a nonzero temperature the long range order is destroyed when the energy of thermal fluctuations is large enough to damage the correlation of the neighbor defects.

The long range magnetic order was not observed downto 1.2 K for pure samples which showed the diminishing of the susceptibility below T_{SP} for more than 10 times. Nevertheless the pure crystals of $CuGeO_3$ demonstrate unusual magnetic properties at low temperatures. The low temperature study of the electron spin resonance (ESR)[11,12] showed that the ESR spectrum is complicated by splitting into several components of the unknown nature. The effect of the electric field influence on the magnetic susceptibility in the temperature range of the residual susceptibility[13] also indicate the unusual state of the crystal at low temperatures. The residual susceptibility was supposed to be provided by the magnetic defects which arise together with the lattice defects at the temperature T_{SP}, these defects being the boundaries of the spin-Peierls crystallites. The crystallites differ through the different values of the phase of the dimerization. Thus the residual susceptibility may arise in a rather pure crystal and may exceed the susceptibility of the paramagnet with the number of magnetic ions equal to the number of defects in the high temperature phase.

The aim of the present paper is the study of the ESR spectra of the pure monocrystals of $CuGeO_3$ for the determination of the structure of the magnetic defects of the spin-Peierls phase.

II. EXPERIMENTAL TECHNIQUES AND SAMPLES

The crystals of $CuGeO_3$ were grown from the high purity components by means of the spontaneous crystallization from the flux melt at the slow cooling. The velocity of the crystallization was 10^{-3}cm/hour. The test of the impurities content was performed by means of the activation analysis and by atomic plasma spectroscopy (ICP/APS). The concentrations of the impurities Fe, Ni, Mn, Co did not exceed 10^{-4} per Cu-ion.

The magnetic impurities and defects provide the residual magnetic susceptibility in the spin-Peierls crystal. Therefore the quality of the crystal may be characterized by the ratio Q of the susceptibility at 15 K to the minimal value of the susceptibility measured at 5 K. The smaller is the amount of the defects in the spin-Peierls crystal, the higher is the value of the quality factor Q. For the main set of our samples Q =20.

Samples from other growth procedures were also studied for the comparison of the samples with the different content of the different defects. ESR spectra of the samples used in[12] (sample N2) were taken. This sample was prepared by the floating zone method and contained the impurity of Fe in the amount of 10^{-3}. The quality factor of this sample is 7. A set of samples was grown from the same initial materials as the main set but at the more rapid crystallization rate for the comparison of the samples with different concentrations of the structure defects. The crystallization rate for these samples was 1cm/hour and the value of Q was 6. The samples grown at the rate of the crystallization 6 cm/h had the value of Q=3. For the investigation of the impurities influence on the ESR signal the samples doped with Ni of the composition $Cu_{0.995}Ni_{0.005}GeO_3$, were grown at the rate 1 cm/h.

The lines of the magnetic resonance were taken as the dependencies of the microwave power transmitted through the cavity containing the sample vs the magnetic field in the frequency range 18-75 GHz. The spectrometer with the modulation of the magnetic field was used at the frequency 9 GHz and the field-derivatives of the magnetic resonance lines were recorded. The measurements were done in the temperature interval 1.2-25 K in the magnetic fields up to 60 KOe.

III. THE SPECTRUM OF THE MAGNETIC RESONANCE

At the temperatures above and in the vicinity of T_{SP} the ESR spectrum of $CuGeO_3$ consists of a single line. As described in[11,12], this line broadens at the diminishing of the temperature and further the spectrum splits at 5 K, there arise four strong and several weak lines at lower temperatures.

The low temperature ESR signals are relatively weak. Using the known value of the molar susceptibility of $CuGeO_3$ at T=15 K and the value of Q-factor one could estimate the effective concentration of the paramagnetic defects which could be responsible for the ESR signal of the observed intensity. The main set samples integral intensity at 5 K is $1.0{\cdot}10^{-3}$ of the intensity of the electron spin resonance of the paramagnet with one electron spin per Cu-ion.

The characteristics of the magnetic resonance are shown in figures 1-6.

The evolution of the lineform with temperature and the transformation of one single line into four lines is shown on the Fig.1. One could see here the part of the integral intensity of the broad line is splitting and forms a new line on the right side of the main line at T=3.5 K, the main line is also splitting into three components.

Fig.2 shows the records of the magnetic resonance spectra at $\mathbf{H} \parallel c$ at different frequencies taken at the temperature 1.3 K. The main four lines are marked here by the numbers 1,2,3,4. The weaker lines are marked by the letters $\alpha, \beta\, \gamma, \epsilon, \nu$. The dependencies of the resonant frequencies on the magnetic field $f_i(H)$ for $\mathbf{H} \parallel c$ are illustrated on Fig.3. The subscript i corresponds to one of the lines marked by numbers and letters on Fig.3. Three close lines 1,2,3 has frequency-field dependencies in the form of three parallel straight lines. The middle straight line of the resonance 2 passes through the origin of coordinates. The frequency-field dependence of the resonance line 4 is a straight line with another slope and also passes trough the origin of the coordinates. The frequencies $f_{1,2,3,4}$ don't depend on the temperature in the range 1.3-4 K. The data shown on Fig.3 and the measurements at $\mathbf{H} \parallel a$, $\mathbf{H} \parallel b$ show that the dependencies $f_{1,2,3,4}(H)$ for the principal orientations of the magnetic field and within the frequency interval 9-75 GHz are following:

$$f_i(H_\kappa) = \frac{\mu_B}{2\pi\hbar} g_{i\kappa} H_\kappa + d_{i\kappa} \qquad (2)$$

Subscript κ denotes one of the field directions along the axes a, b or c. The values of $g-$factors $g_{i\kappa}$ and of the constants $d_{i\kappa}$ are given in the Table 1. The nonzero values of $d_{1\kappa}$, $d_{3\kappa}$ describe the splitting of the magnetic levels at the zero field. The zero field splitting has the maximum value for $\mathbf{H} \parallel b$ and vanishes at $\mathbf{H} \parallel a$.

Table 1

i	g_{ia}	g_{ib}	g_{ic}	d_{ia}, GHz	d_{ib},GHz	d_i,GHz
1	2.17	2.26	2.10	0.0	-1.7	1.15
2	2.17	2.26	2.10	0.0	0.0	0.0
3	2.17	2.26	2.10	0.0	2.05	-0.95
4	1.82	1.86	1.43	0.0	0.0	0.0

The representation of the spectrum in the field range covering the lines 1,2,3,4 in the form of four lorentzian lines revealed the presence of the fifth line which has the $g-$factor of about 2.0 and the linewidth of about 600 Oe. The presence of this fifth line (we note it by the number "0") is obvious e.g. at the Fig.2 where the up and down displacements from zero line of the 9GHz-record of the derivative are observable at the resonant fields of the resonances 1,2,3. These displacements correspond to the presence of a wide line in addition to lines 1,2,3,4. The intensity of the line "0" is about 0.07 of the integral ESR intensity at 1.3 K for the sample with Q=20. For the sample with Q=6 the intensity of the line "0" is much larger and exceeds for 10 times the total intensity of lines 1,2,3,4.

The dependencies of the resonant field on it's orientation are given in the Fig.4. The lines 1 and 3 exchange their positions so that the frequency diffferences $f_{1,3} - f_2$ change their signs. The rotation of the field from the $c-$ direction to $a-$direction results in the merging of the lines 1,2,3 into one line. The resonance line 4 has a strongly anisotropic $g-$factor with the variation between the limits 1.43 and 1.86 depending on the orientation of the magnetic field with respect to crystal axes.

The line α was observable only on the frequencies 9.1 and 9.4 GHz. The difference of the resonance field values for these frequencies shows that this line has the zero frequency in zero field and the $g-$factor value of 5.4 at $\mathbf{H} \parallel c$. The value of the $g-$factor of the line β doesn't depend on the orientation of magnetic field and is equal to 4.21. This value is typical for the Fe^+ - ion[14]

Fig.5 shows the temperature dependence of the integral intensity of the ESR spectrum and of the intensity of lines 3 and 4 on the frequency 9.4 GHz. The dependencies of the linewidths on temperature are shown in Fig.6. At the temperature 5 K, where the splitting into four lines occurs, the peak of the linewidth for all lines takes place.

The comparison of the ESR lines of the samples of different quality is presented on Fig's. 7,8 and in the Table 2. For the samples with the smaller Q-values the intensity of the line "0" is larger. This fact is illustrated in Table 2 by the ratio $\sum_{1-4}/I_0$ of the total intensity of lines 1,2,3,4 to the intensity of the line "0" at T=1.3 K. Besides the data of the present work the data from the paper[11] are also given. For the low-Q samples the intensity of the line "0" becomes larger, and the lines 1,2,3 broaden or disappear as observed in crystals grown at the higher crystallization rate. The line 4 is also broadened and at the same time enlarged in the intensity. The comparison of the samples from the main set and of the sample N2 from[12] shows that the low-Q sample has the stronger line 2. The lines 1 and 3 have the same intensity and the linewidth as in the pure sample. The line α is of the same intensity as in the most pure sample, and the line β is more intensive according to the data of the Fe-concentration analysis.

The Fig.8 shows that the smaller is the crystallization rate the smaller is the intensity of the line 4. This observation is made for the samples grown from the same initial components and confirms the arising of line 4 from the structure defects within the magnetic subsystem of Cu-ions rather than from impurity atoms.

Table 2

N	v_{cr}, cm/h	$C_{Ni,Co,Mn}$	C_{Fe}	Q	$\sum_{1-4}/I_0$	T_{SP}	
1	10^{-3}	$<10^{-4}$	$<10^{-4}$	20	15	14.5	
2	1	$<10^{-4}$	$<10^{-4}$	6	0.1	14.0	
3	6	$<10^{-4}$	$<10^{-4}$	3	0.01	13.0	
4	0.1	$<10^{-4}$	$5\cdot10^{-4}$	7	1	14.5	[12]
5	unknown	unknown	unknown	100	20	14.5	[11]
6	1	$5\cdot10^{-3}$ (Ni)	$<10^{-4}$	2		12.5	

IV. NONLINEAR MAGNETIC RESONANCE

The resonant microwave magnetic susceptibility appeared to be power-dependent for the line 4. Fig.9 shows the lines of the magnetic resonance absorption on the frequency 20.2 GHz at different levels of the incident microwave power. When the microwave power exceeds some threshold value the enlarging of the susceptibility occurs and the intensity of the line 4 becomes larger than the total intensity of lines 1,2,3. The lineform becomes asymmetric, the additional absorption on the left wing is more elongated then on the right wing.

The dependence of the imaginary part of the susceptibility on the microwave power is shown on Fig.10 for the case of the resonance field value and for the wing of the resonance curve. This dependence demonstrates the threshold for the enlarging of the susceptibility. The threshold power, marked by the arrow on the figure, corresponds to the incident microwave power of about 1 mW and to the absorption in the sample of about 100μW. The strength of the microwave magnetic field on the sample is about 0.1Oe.

The effect of the nonlinear enlarging of the imaginary part of the microwave magnetic susceptibility has the maximum value at the frequency about 20 GHz. At the frequencies 18 and 23 Ghz this effect also is present but the nonlinear enlarging of the susceptibility at the comparable power is approximately 3 times smaller. For other frequencies (the closest of them is 26 GHz) the nonlinear enlarging of the susceptibility is not larger then the noise level.

V. DISCUSSION

A. Temperature evolution of the lineform

The temperature evolution of the magnetic resonance lineform i.e. the transformation of the single narrow line into the single wide line and then into four narrow lines arisen from this wide line may be explained by taking into account the exchange interaction of the paramagnetic defects of the spin-Peierls phase with the thermally activated triplet excitations[11]. The exchange frequency is determined as the product of the exchange integral expressed in the frequency units by the relative concentration of the triplet excitations[15]. When the exchange frequency is greater than the difference of the frequencies of the different resonance lines, only single line with some average frequency should be observed (the effect of the exchange narrowing). By lowering the temperature the concentration of triplets drops and when the exchange frequency passes the value of the order of frequencies difference the separate lines arise which are narrowing at the further freezing out of the triplet excitations[16].

This scenario of the lineform evolution was observed in the TCNQ organic crystals, having the nonmagnetic ground state and the triplet excitations states[16]. In the pure crystals of this substance the line widening and splitting into two lines were observed. These two lines corresponded to the triplet excitations with the effective spin $S = 1$ in the crystal field. The line corresponding to the residual defects with the effective spin $S = 1/2$ was found in the irradiated crystals of TCNQ[17]. The two lines corresponding to $S = 1$ vanish in intensity with temperature. For the crystals containing defects the lines attributed to $S = 1/2$ and $S = 1$ do not disappear at the temperature diminishing and show the temperature dependence of the intensity like the intensity of a paramagnetic sample ESR. It was shown in[11], that the linewidth of the ESR in $CuGeO_3$ follows the temperature dependence provided by the described mechanism in the range of the rapid (above 5 K) as well as in the range of the slow (below 5 K) exchange.

B. Effective spin and the origin of the defects

In the temperature range below 4 K the susceptibility is suppressed by the transition into the spin-Peierls phase, the ground state of this phase is singlet and nonmagnetic, the excitation states being separated by the energy gap. The magnetic susceptibility and the intensity of the ESR signal should be exponentially close to zero at low temperatures. The nonzero susceptibility and the ESR signal are provided by the defects of the spin-Peierls phase. Clearly the observed ESR signals are attributed to different type of defects and further we try to identify these defects.

The lines 1,2,3 have equal $g-$factor values, close to the $g-$factor of the Cu^{2+}-ions in the paramagnetic phase of $CuGeO_3$. This fact shows that the lines 1,2,3 are attributed to Cu-ions. The value of the $g-$factor of the line 4 differs strongly from the Cu^{2+} $g-$factor value. One could assume this line to be provided by impurity. But the chemical composition analysis gave the limit of the paramagnetic impurities concentration corresponding to only a half of the observed magnetic resonance intensity. We recorded the ESR spectrum of the single crystal with the composition $\mathrm{Cu}_{0.995}\mathrm{Ni}_{0.005}\mathrm{GeO}_3$. The impurity ESR line of this crystal corresponds to the g-factors g_a=1.92, g_b=2.00, g_c=1.7, i.e. it's frequency differs sufficiently from the frequency of line 4. Thus the presence of the nickel impurity could not explain this signal. The magnetic resonance signals provided by the nonmagnetic doping do not show $g - factor$ changes above 3%[19]. Besides that the difference in the intensities of the line 4 of the samples prepared at different crystallization rates from the same components testifies the origin of this line from Cu-ions. Thus the results obtained demonstrate that the resonance lines 1,2,3,4 arise from the Cu-ions.

The relative intensity of the line 2 with respect to the lines 1,3 is different for the samples of different quality (see Fig.7). The ratio of the intensities of lines 1 and 3 is the same for different samples. From this fact we conclude that the lines 1,3 are provided by the defects of certain type, and the line 2 arises from the defects of another type. The absence of the crystal field splitting for the line 2 shows the effective spin S =1/2 of this type of defects[20].

The zero field splitting and the angular dependence of lines 1,3 with the exchange of their mutual positions mean that these lines belong to the defects with the effective spin S =1. The splitting of the magnetic resonance line by the crystal field into two lines is characteristic for spin S =1. The angular dependencies of these two lines resonance fields are analogous to the dependencies shown in Fig.5, the separation between the lines being independent on frequency when $g\mu_B H \gg D$, here D is the single ion anisotropy constant of the spin-Hamiltonian.[20]. Therefore we assume that the lines 1 and 3 are concerned with the exchange-coupled $S = 1$ pairs of Cu-ions. The ESR-line of these pairs may be split by the dipole-dipole interaction or by the anisotropic exchange[21]. Such a splitting was observed in the ESR spectrum of copper-acetat-monohydrat[21]. The consideration of dipole-dipole interaction or of the anisotropic exchange is necessary because the splitting of the spectrum of the pairs of $S = 1/2$-ions by the single ion anisotropy is absent.

C. Intrinsic defects of the spin-Peierls phase

We found in our experiments that the line 2 of the $S = 1/2$- and the lines 1,3 of the $S = 1$-defects have the comparable intensities. For the random distribution of the small number of the defects the exchange coupled pairs resonance should be much less intensive than the resonance of the isolated defects. For an explanation of this contradiction one should consider the structure of the magnetic defects of the spin-Peierls crystal arising at the transition point.

As it was described in the Introduction, the low temperature phase is characterized by one of the two values of the dimerization phase. The creation of the domains (crystallites) with the different values of this parameter is possible during the transition. On a boundary between two crystallites the value of ψ changes from $\psi = 0$ to $\psi = \pi$ and at least one atomic layer remains undimerized. The boundaries of the crystallites are usually pinned at the defects and thus one point defect in the high temperature phase may produce the entire plane of the magnetic defects below the transition. The known boundaries of the antiferromagnetic domains are examples of the plane-type defects in a relatively perfect crystal[22]. Fig.11 shows schematically the Cu-ions in the dimerized crystal containing two domains. The orientation of the plane parts of the boundary is chosen to be directed along the principal directions. The boundary of the first type (I) lies in the plane ac and contains the undimerized chains oriented along c-axes coupled by the weak ferromagnetic exchange J_a. The passing of this boundary violates the order of the oxygen atoms displacement. In the second type of boundaries (II), lying in the plane bc (not shown in the Fig 11.) the undimerized spin chains are coupled by the weak antiferromagnetic exchange J_b. In both cases there is a strong intrachain exchange interaction characterized by the exchange integral J_c. The violation of the order of joining of Cu-ions into pairs takes place in the boundaries of the third type (III) lying in the planes ab or in the family of the planes $\{101\}$. This type of boundaries contains the undimerized spins from different chains. The week exchange interactions J_a and J_b are coupling the spins in the plane of this boundary.

The type I boundary contains the magnetically unordered spin chains with the strong intrachain exchange J_c. The week ferromagnetic exchange acts in the perpendicular direction. The magnetic susceptibility of these chains is suppressed by the strong exchange J_c and is of about 1/200 of the susceptibility of the same amount of paramagnetic spins at T =1.5 K. The structure defects in this boundary (vacancies cutting the chains or the steps) should result with a high probability in the creation of $S = 1$ exchange coupled pairs of the Cu-ions due to the ferromagnetic exchange J_a between the spins of the neighboring chains. The breaks of the chains in the boundaries of the type I are probably the sources of the exchange coupled pairs giving the ESR lines 1 and 3.

The angular and frequency dependencies of the magnetic resonance field of lines 1 and 3 may be described on the base of the spin-Hamiltonian of the effective spin $S = 1$[20]:

$$\mathcal{H} = g_c\mu_B H_c + g_b\mu_B H_b + g_a\mu_B H_a + D_c\hat{S}_c^2 + D_b\hat{S}_b^2 + D_{cb}(\hat{S}_c\hat{S}_b + \hat{S}_b\hat{S}_c) \qquad (3)$$

with the parameters $g_c = 2.10$, $g_b = 2.26$, $g_a = 2.17$, $D_c = 0.04$ K, $D_b = -0.05$ K, $D_{cb} = -0.03$ K

The analogous defects in the main spin-Peierls matrix or in the boundaries of the types II and III remain mostly unpaired or create pairs with the spin $S = 0$ due to the stronger antiferromagnetic exchanges along the axes c and b.

The resonance line 2 is naturally combined with the isolated breaks of the spin chains away from the boundaries or in the boundaries of the type II. These breaks produce the free $S = 1/2$ spins.

The splitting of the ESR line into three spectral components at lowering the temperature was also observed in the organic spin-Peierls crystals[23]. In this case the analysis of the angular- and frequency-dependencies of the resonant fields of theses components was not performed. The authors interpreted the observed components as ESR signals of different magnetic ions with different $g-$factors.

The specific transformation of the ESR line in the spin-Peierls magnet with the splitting of the single line into several lines and among them a triplet was confirmed by the observation of the described scenario of the evolution of the lineform for the lately discovered second inorganic spin-Peierls crystal NaV_2O_5[24].

D. Magnetic clusters in the spin-Peierls matrix

We consider now the domain boundaries of the type III, having the undimerized spins from different chains in the plane. According to the concept developed in[7,10] each undimerized spin is a center of a region with the antiferromagnetically correlated spins. The size of this region (soliton) is estimated theoretically as about 7 lattice periods along the $c-$axes. The total spin of the soliton is 1/2 and the average of the spin projection on the site diminishes with going away from the undimerised spin due to the dimerization (see Fig. 12).

These objects are magnetic clusters within the nonmagnetic spin-Peierls matrix. Magnetic resonance of this clusters having the internal structure is an yet unsolved problem. The related problem of magnetic resonance of the three-spin cluster of equal $S = 1/2$ ions is reported[25]. For the isosceles triangular cluster with the small deviation from the equilateral triangle the energy levels are given by the relation:

$$\begin{aligned} E_{1,2,3,4} &= \pm\tfrac{1}{2}(G^2 + \delta^2 + g^2\mu_B^2 H^2 \\ &\pm 2g\mu_B H(\delta^2 + G^2\cos^2\theta)^{1/2})^{1/2} \end{aligned} \tag{4}$$

here θ - is the angle between the z -axes of the cluster symmetry and the magnetic field, $J_{0,1}$ -exchange integrals, $\delta =\mid J_1 - J_0 \mid$, G- coefficient of the antisymmetric exchange interaction of Dzyaloshinski-Moria. The coefficient G equals zero if the symmetry center exist between the ions constructing the pair. If the energies of transitions between the levels (4) are small compared to δ, G then they are determined by the relation

$$\hbar\omega = \frac{g}{\sqrt{1 + G^2\cos^2\theta/\delta^2}}\mu_B H \tag{5}$$

Thus in the low-frequency range the spectrum of the magnetic resonance of the triangular cluster is analogous to the ESR spectrum of an isolated single ion with the strongly anisotropic $g-$factor and with $g_z < 2$. The experiments with the organic complex crystals containing the triades of Cu-ions revealed the correspondence of the static magnetic susceptibility[27] and of the resonant properties[26] to the consideration described above, considering the nonzero value of G.

For the description of the linear three-spin cluster created within the nonmagnetic spin-Peierls matrix around an undimerized spin we take the Hamiltonian in the form:

$$\begin{aligned} \mathcal{H} = J_{12}\hat{\mathbf{S}}_1\hat{\mathbf{S}}_2 + J_{23}\hat{\mathbf{S}}_2\hat{\mathbf{S}}_3 + J_{13}\hat{\mathbf{S}}_1\hat{\mathbf{S}}_3 + \mathbf{G}_{12}[\hat{\mathbf{S}}_1\hat{\mathbf{S}}_2] \\ + \mathbf{G}_{23}[\hat{\mathbf{S}}_2\hat{\mathbf{S}}_3] \end{aligned} \tag{6}$$

here $\mathbf{G}_{12}$ and $\mathbf{G}_{23}$ are vector parameters of the Dzyaloshinski-Moria-interaction. The energies of the two lowest states of the cluster at the arbitrary orientation of the magnetic field are given by the relation:

$$\begin{aligned} E_{1,2} = \tfrac{\varepsilon_1+\varepsilon_2}{2} - \tfrac{1}{2}[(\varepsilon_1 - \varepsilon_2)^2 + \mathbf{G}^2 + (\mathbf{h})^2 \\ \pm 2((\varepsilon_1 - \varepsilon_2)^2\mathbf{h}^2 + (\mathbf{hG})^2)^{1/2}]^{1/2} \end{aligned} \tag{7}$$

here ε_1 , ε_2 are the energies of the two possible $S = 1/2$ states of the cluster in the absence of the antisymmetric exchange and of the magnetic field:

$$\begin{aligned} \varepsilon_{1,2} &= -\tfrac{1}{4}(J_{12} + J_{13} + J_{23}) \\ &\pm \tfrac{1}{2}\sqrt{\left[J_{23} - \tfrac{1}{2}(J_{12} + J_{13})\right]^2 + \tfrac{3}{4}(J_{12} - J_{13})^2} \end{aligned} \tag{8}$$

$\mathbf{G}$ and $\mathbf{h}$ are $\mathbf{G} = \frac{\mathbf{G}_{12}+\mathbf{G}_{23}}{\sqrt{3}}$, $\mathbf{h} = g\mu_B\mathbf{H}$, g takes the values of the corresponding components of the $g-$tensor of the single Cu-ion.

For the case $\mathbf{h} \perp \mathbf{G}$ the effective $g-$factor is approximately given by

$$g_{eff} = g\left[1 - \frac{G_x^2 + G_y^2}{2(\varepsilon_2 - \varepsilon_1)^2}\right] \tag{9}$$

Taking $J_{23} = J_{12} = 10$ meV[3], $J_{13} = 3.6$ meV[28] we obtain for the observed $g = 1.43$ that the vector $\mathbf{G}$ should be perpendicular to the plane of the fragment CuO_2-CuO_2-Cu with the value of $G_{12} + G_{23}$ of about 8 meV. Note that $\mathbf{G}$=0 for the cluster with the center of symmetry at the middle spin. However, as it is seen from Fig.11 there is no symmetry centers on the sites of the undimerized spins within the boundary of the type III. The symmetry centers disappeared due to the distortions of the regular dimerized pattern for the neighboring pairs of the Cu-ions.

The estimation of the antisymmetric exchange given above is of the order of the main exchange interaction which seems to be nonrealistic. Further we consider the five spin model (Cu5-Cu4-Cu1-Cu2-Cu3). Here the number of the states with the total spin $S = \frac{1}{2}$ which are admixed to the main doublet by the antisymmetric exchange is enlarged. As a consequence the relation (9) transforms in the following way:

$$g_{eff} = g[1 - \frac{(\mathbf{G_{12}+G_{23}+G_{41}+G_{54}})^2}{3E^2_{31}} - \frac{(\mathbf{G_{12}+G_{23}-G_{41}-G_{54}})^2}{12E^2_{21}}] \qquad (10)$$

here E^2_{31} and $^2_{21}$ are determined by the equations:

$$^2_{21} = [J_{23} - \frac{1}{2}(J_{12} + J_{13}) + \frac{1}{4}J_{24}]^2 + \frac{3}{2}(J_{12} - J_{13})^2 \qquad (11)$$

$$\begin{aligned} E^2_{31} = \quad & \{J_{23} - \tfrac{1}{2}(J_{12} + J_{13}) - \tfrac{3}{4}J_{24} + \\ & [(J_{23} - \tfrac{1}{2}(J_{12} + J_{13}) + \tfrac{1}{4}J_{24})^2 + \\ & \tfrac{3}{2}(J_{12} - J_{13})^2]^{1/2}\}^2 + \tfrac{3}{2}(J_{12} - J_{13})^2 \end{aligned} \qquad (12)$$

Note that only the antisymmetric term $G_{12} + G_{23}$ is included in (9) while the symmetrical contribution $G_{12} + G_{23} - G_{41} - G_{54}$ arises in (10). This principal difference is due to the fact that the three-spin cluster has the single excited state with the total spin $S = \frac{1}{2}$ and this state is antisymmetric. There are the symmetric as well as antisymmetric with respect to the center of the cluster states among the $S = \frac{1}{2}$ excited states of the five-spin cluster. Therefore both the antisymmetric and the symmetric combinations $G_{12} + G_{23} + G_{41} + G_{54}$, $G_{12} + G_{23} - G_{41} - G_{54}$ contribute to the change of $g-$factor.

The five spin cluster has four $S = \frac{1}{2}$ excited states. The relation (10) takes into consideration only two lower states otherwise the formula becomes too cumbrous. The calculation under the assumption $G_{12} = G_{23} = G_{54} = G_{41}$ results in g_c=1.5 at the modulus of G_{12} equal to 2.9 meV. The following numerical data are used here: $J_{12} = J_{14}$ =10 meV, $J_{23} = J_{45}$ =10.4 meV (dimerized spin pairs), $J_{13} = J_{15}$ =3.6 meV.

The numerical calculations performed by the exact diagonalization of the energy matrixes in the presence of the magnetic field including all the excited states of the five spin cluster give G_{12} = 3.0 meV.

The average values of the spins projections of the spins of the cluster obtained during the process of this calculation are given in Fig.12. The presence of the antisymmetric exchange in CuGeO$_3$ with the Dzyaloshinsky vector perpendicular to the $c-$direction was at first assumed in[29] at the analysis of the reasons of the high-temperature ESR line broadening. It was noted that this assumption contradicts to the crystal structure of the CuO$_2$-chains reported in[2]. We note here, that the symmetry is lowered in the vicinities of the undimerized spins contained within the domain boundaries of the type III and the presence of the Dzyaloshinski-Moriya interaction becomes permitted at least below T_{SP}.

The ESR line 4 is obviously to be associated with the defects of the last type of the Cu-ions magnetic system. The consideration of five-spin-cluster given above enables one to explain the strong deviation of the $g-$factor from the value 2.0 and the strong anisotropy of $g-$ factor by taking into account the antisymmetric exchange interaction with the parameter of about 0.3 of the exchange integral.

Surely the above consideration of the magnetic cluster with the internal structure defined by the Dzyaloshinsky-Moriya interaction give only qualitative explanation of the strong deviation of $g-$factor. There are two following contradictions of the described model to the experimental facts. At first, the value of $g-$factor does not come close to 2.0 for any direction of the magnetic field (there should be such a direction according to the model), and secondary - the strong diminishing of $g-$factor is to be for any direction perpendicular to $\mathbf{G}$ but we observe the strongest diminishing only along $c-$axes. Probably these discrepancies may be ascribed to the antisymmetric exchange of the next-nearest-neighbor-ions or to the nonparallel Dzyaloshinsky vectors of the different pairs of ions.

The 9 GHz-ESR of the crystal of higher quality was reported in[11]. The data given there testify the Q-value of about 100. The ESR lines $\alpha, 1, 2, 3, 4$ were also observed there and the resonance fields of these lines correspond well to the fields observed in the present paper. This fact confirms that the spectrum consistent from a triplet line and of the cluster line is characteristic for pure spin-Peierls crystals.

E. 2D-magnet on the boundary between the domains of the spin-Peierls phase

The localized soliton may be considered as a magnetic quasiatom because it's internal structure is fixed by the strong exchange J_c. Thus the type III boundary is a two-dimensional-magnet of these quasiatoms, coupled by the ferromagnetic exchange NJ_a along $a-$direction and by the antiferromagnetic exchange NJ_b along the $b-$axes. Here N is the effective number of spins within the quasiatom. Using for an estimation $N \approx 5$ we derive the exchange integrals between quasiatoms of about 50 K along b and about -5 K along $a-$axes. Due to the anisotropy energy of per quasiatom-spin of E_a=0.5 K, the ordering temperature of this 2D-magnet is of about

$T_c \approx N(J_bJ_a)^{1/2}/ln(NJ_b/E_a) \approx 3K$

Therefore at the temperature of our experiments when $T \ll NJ_b$ this planar magnet may be unordered but strongly correlated magnet. The long-wave excitations of this magnet are analogous to spin waves in the antiferromagnet without anisotropy.[30]. One of the branches of these excitations spectrum $\omega_{1\mathbf{k}}$ is gap-less even in presence of the magnetic field. The second branch has the gap $\omega_{20} = g_\alpha \mu_B H_\alpha$. The uniform high frequency magnetic field enables us to excite the uniform precession mode with the frequency ω_{20}. Because of the elliptical trajectories of the spin precession caused by the anisotropy, the parametric excitation of the pairs of spin waves of the gap-less mode is possible by the decay of the uniform mode, when the pair meets the condition of the parametric resonance:

$$\omega_{mw} = \omega_{1\mathbf{k}} + \omega_{1-\mathbf{k}} \tag{13}$$

Here ω_{mw} is the frequency of the microwave pumping. The absorption of energy at the parametric excitation has a threshold in pumping power, the flow of energy into the spin-wave modes having the resonance maximum near the frequency of the uniform mode (see, e.g.[31,32]). The resonance is due to the transfer of energy via the magnetization oscillation of the gap-like-mode.

The parametric excitation of the spin waves of the gap-like mode should provide the absorption of the microwave magnetic field energy in the field range below the resonance field of the uniform precession at a half frequency. We observed such absorption bands, as is it seen on Fig.2 and Fig.3 (line ν).

The observed effect of the threshold enlarging of the susceptibility at the resonance of the line 4 leads one to the conclusion that there are the two dimensional planar magnetic defects inside the spin-Peierls matrix. The point-like magnetic defects could not provide the nonlinear effect with the enlarging of the susceptibility, only the saturation effect is known for the magnetic resonance of the isolated ions, with the diminishing of the imaginary part of the susceptibility at enlarging microwave power. The presence of the three-dimensional magnetically correlated areas is less probable because 3D-ordering temperature should be greater, of the order of $(J_c J_b)^{1/2} \geq$ 10K and the 3D-dimensional order would result in the observable zero-field gaps for both branches of the spectrum. This assumption is in a contradiction with the linear and gapless dependence $f_4(H)$.

VI. CONCLUSION

The defects of the spin-Peierls phase with the effective spins 1/2 and 1 are identified on the base of the analysis of the low temperature ESR spectra of pure crystals of $CuGeO_3$. Spin-1/2-defects are created by the breaks of the spin chains and spin-1-defects - by the exchange coupled pairs of this breakups placed in the boundaries of the domains of the spin-Peierls phase.

The additional ESR signal is found revealing the two-dimensional magnetic defects with the long-range magnetic correlations. This planar objects are proposed to be the boundaries of the spin-Peierls phase with the different values of the dimerization phase.

VII. ACKNOWLEDGMENTS

The authors are indebted to L.A.Prozorova, V.A.Atsarkin, V.V.Demidov, I.A.Zaliznyak, V.A.Marchenko, S.S.Sosin, L.E.Svistov and H.Benner for valuables discussions, H.-A.Krugg von Nidda for taking part in the measurements at the frequency 9 GHz, Yu.M.Tsipenyk, V.I.Firsov and M.Fedoroff for the element analysis of the samples.

The work is supported by the Russian Foundation for Fundamental Research (project 98-02-16572) and by the Civilian Research and Development Foundation (project RP 1-207). The measurements on the frequency 9GHz are made in Technische Hochschule Darmstadt, Germany supported by Sonderforschungbereich 185.

---

[1] M.Hase, I.Terasaki, K.Uchinokura, Phys.Rev.Lett. **70** 3651 (1993)

[2] K.Hirota, D.E.Cox, J.E.Lorenzo, G.Shirane, J.M.Tranquada,
M.Hase, K.Uchinokura, H.Kojima, Y.Shibuya, I.Tanaka, Phys.Rev.Lett. **73** 736 (1994)

[3] L.-P.Regnault, M.Aïn, B.Hennion, G.Dhalenne, A.Revcholevschi, Phys.Rev.B **53** 5579 (1996)

[4] J.W. Bray, H.Hart, L.Interrante, I.Jacobs, J.Kasper, G.Watkins, S.Wee, J.Bonner, Phys.Rev.Lett. **35**, 744, (1975).

[5] L.N. Bulaevskii, Sov.Phys. Solid State **11**, 921 (1969)

[6] H.Bethe, Z.Phys **71**, 205 (1931)

[7] D.Khomskii, W.Geertsma and M.Mostovoy, Proceedings of the 21-st International Conference on Low Temperature Physics, Prague 1996. Chech. J. Phys. **46** Suppl.S6 3239 (1996)

[8] J.G.Lussier, S.M.Coad, D.F.McMorrow, D.Paul, J.Phys.Condens.Matter **7** L325 (1995)

[9] L.-P.Regnault, J.-P.Renard, G.Dhallenne, A.Revcholevschi,
Europhys.Lett. **32** 579 (1995)

[10] H.Fukuyama, T.Tanimoto, M.Saito, J.Phys.Soc.Japan **65** 1182 (1996)

[11] M.Honda, T.Shibata, K.Kindo, Sh. Sugai, T.Takeuchi, H.Hori, J.Phys.Soc.Jpn. **65** 691 (1996)

[12] A.I.Smirnov, V.N.Glazkov, A.N.Vasil'ev, S.M.Coad, D.McK.Paul, G.Dhalenne, A.Revcholevschi, JETP Lett. **64** 305 (1996)

[13] A.I.Smirnov, A.N.Vasil'ev, L.I.Leonyuk, JETP Lett. **64** 695 (1996)

[14] S.A.Altshuler, B.M.Kosyrev, Electron Paramagnetic Resonance, Moscow, "Nauka" 1972 (in russian) page 429

[15] M.T.Jones, D.B.Chesnut, J.Chem.Phys. **38** 1311 (1963)

[16] D.B.Chesnut, W.D.Philips, J.Chem.Phys. **35** 1002 (1961)

[17] H.M.McConnell, H.O.Griffith, D.Pooley, J.Chem.Phys **36** 2518 (1962)

[18] M.Weiden, W.Richter, C.Geibel, F.Steglich, P.Lemmens, B.Eisener, M.Brinkman, G.Guntherodt, Physica B, **225** 177 (1996)

[19] P.Fronzes, M.Poirier, A.Revcolevschi, G.Dhalenne Phys.Rev.B **56** 7827 (1997)

[20] A.Abragam, B.Bleaney, Electron Paramagnetic Resonance of Transition Ions, v.1, "Clarendon Press", Oxford 1970, chapter 1, section 5.

[21] *ibid*, chapter 9 section 5.

[22] D.N.Astrov, Sov.Phys.JETP **11** 708 1960

[23] I.S.Jacobs, J.W.Bray, H.R.Hart, Jr., L.V.Interrante, J.S.Kasper, G.D.Watkins, D.E.Prober, J.C.Bonner Phys. Rev. B **14** 3036 (1976)

[24] A.N.Vasil'ev, A.I.Smirnov, M.Isobe, Y.Ueda Ph.Rev.B **56** 5065 (1997)

[25] M.I.Belinskii, B.S.Tsukerblat, A.V.Ablov Fiz.Tverd.Tela **16** 989 (1974) (Sov.Phys. Solid State)

[26] Yu.V.Yablokov, V.K.Voronkova, L.V.Mosina, Electron paramagnetic Resonance of the Exchange Clusters, Moscow, "Nauka", 1988
Yu.V.Yablokov,
B.Ya.Kuyavskaya, A.V.Ablov, L.V.Mosina, M.D.Mazus, Dokl.Akad.Nauk **256** 1182 (1981) (Sov.Phys. Doklady)

[27] B.S.Tsukerblat, V.M.Novotvorcev, B.Ya.Kuyavskaya, M.I.Belinskii A.V.Ablov, A.N.Bazhan, V.T.Kalinnikov, Pisma Zh.Eksp.Teor.Fiz **19** 525 (1974) (Sov.Phys. JETP Lett.)

[28] J.Riera, A.Dobry, Ph.Rev.B **51** 16098 (1995)

[29] I.Yamada, M.Nishi, J.Akimitsu, J.Phys.Cond Matt **8** 2625 (1996)

[30] G.Mueller, H.Thomas, H.Beck, J.C.Bonner, Ph.Rev.B **24** 1429 (1981)

[31] V.I.Ozhogin, Sov.Phys. JETP **31** 1121 (1970)

[32] V.V.Kveder,
B.Ya.Kotyuzhanskii, L.A.Prozorova, Sov.Phys. JETP **47** 1165 (1973)

Figure captions

Fig.1. 26.7 GHz magnetic resonance lines taken at different temperatures (field dependencies of the signal of the microwave power detector)

Fig.2. Magnetic resonance lines of $CuGeO_3$ at $\mathbf{H} \parallel \mathbf{c}$, taken at the frequencies 37.0, 18.0, 9.1 GHz and at the temperature 1.2 . For the frequency 9.1 GHz the field-derivative of the ESR line is given.

Fig.3 ESR spectrum at $\mathbf{H} \parallel c$, T=1.3 K. The deviations of the resonant frequency from the line 2 resonance frequency $f = 2.88H$ are given.

Fig.4. Angular dependencies of the ESR field at the frequency 9.4 GHz, T=1.5 K for the rotation of the field in the planes *ac* and *bc*.

Fig.5. The dependence of the integral ESR intensity and of the intensity of the lines 2,3,4 on the temperature for the frequency 9.4 GHz. The numbers indicate the ESR lines according to Fig.2., the integral intensity is marked by the sign $\sum$

Fig.6. The dependence of the ESR linewidth on the temperature for the frequency 9.4 GHz. The numbers are marking the resonant lines according to Fig.2.

Fig.7. Comparison of the absorption line derivatives of two samples with Q =20 and Q =6 at T =1.5 K, on the frequency 9.1 GHz. The samples differ through the Fe-content and the growth methods. The amplitude of the signals is normalized to the equal intensity at T =15K

Fig.8. The comparison of the ESR lines of the samples prepared from the same components at the different crystallization rate. The lines are taken at T = 1.8 K, the amplitude is normalized to equal intensities at 15 K.

Fig.9. The field dependence of the power transmitted through the resonator with the sample at the different microwave incident power values, at the temperature 1.2-1.6 K. $\mathbf{H} \parallel c$, f =20.2 GHz. The power values are given in arbitrary units. The change of the temperature of the resonator is due to the heating by microwave power.

Fig.10. The dependence of the imaginary part of the magnetic susceptibility on the microwave power for the ESR line 4 at the resonant magnetic field (triangles) and at the left wing of the resonant line (squares). P_{cr} and P_{cw} are the threshold values of the power at the resonance and on the wing correspondingly. T =1.5 K. $\mathbf{H} \parallel c$, f =20.2 GHz

Fig.11. Scheme of the domains of the dimerization and of the domain boundaries of types I and III. The filled circles are undimerized Cu-ions.

Fig.12. Proposed average spin projections in the vicinity of the dimerization defect (upper part). Lower part - calculated average values of the spin projections for the five-spin-cluster with the symmetric and antisymmetric exchange.

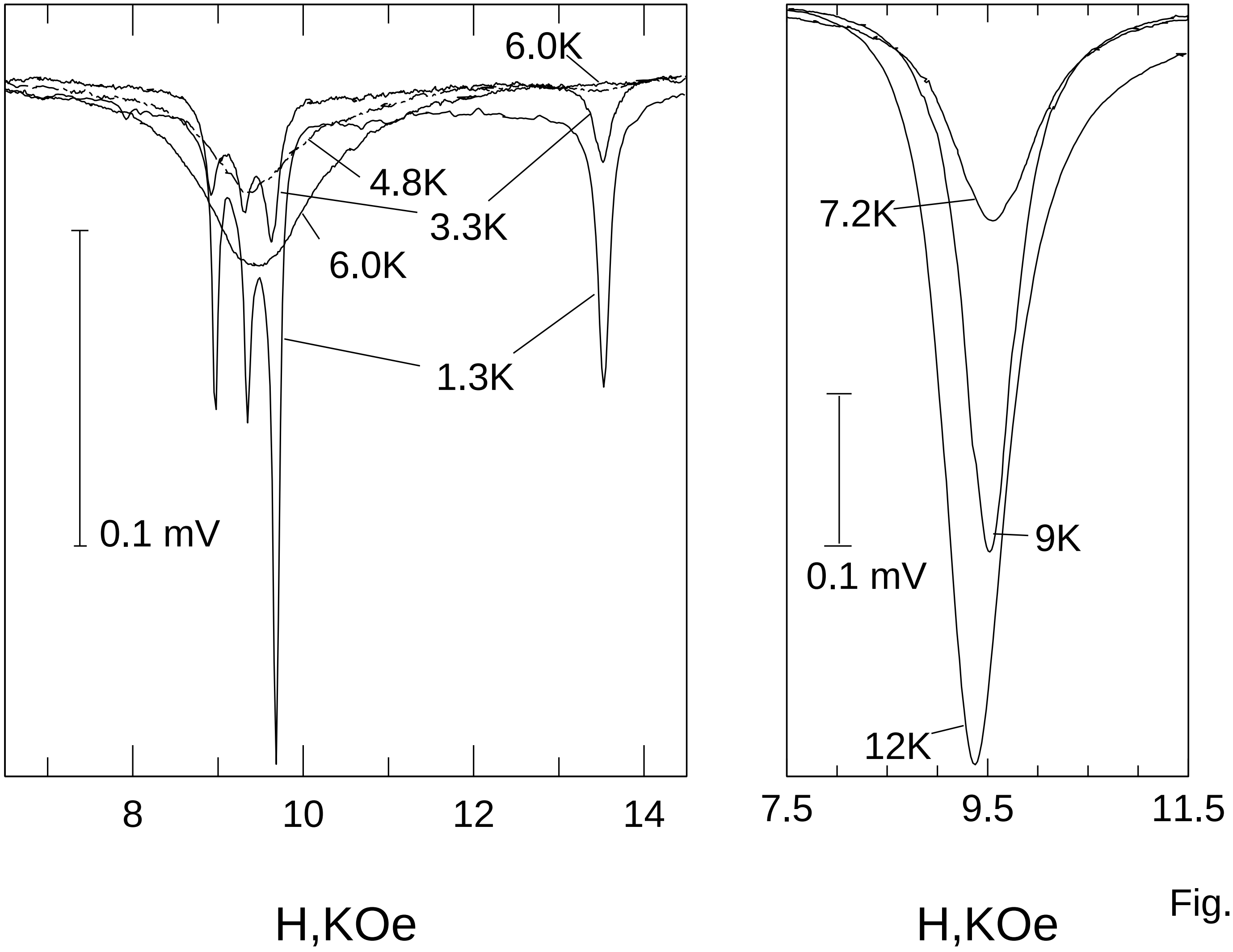
6.0K
4.8K
3.3K
6.0K
1.3K
0.1 mV
8
10
12
14
H,KOe
7.2K
9K
0.1 mV
12K
7.5
9.5
11.5
H,KOe

Fig.1

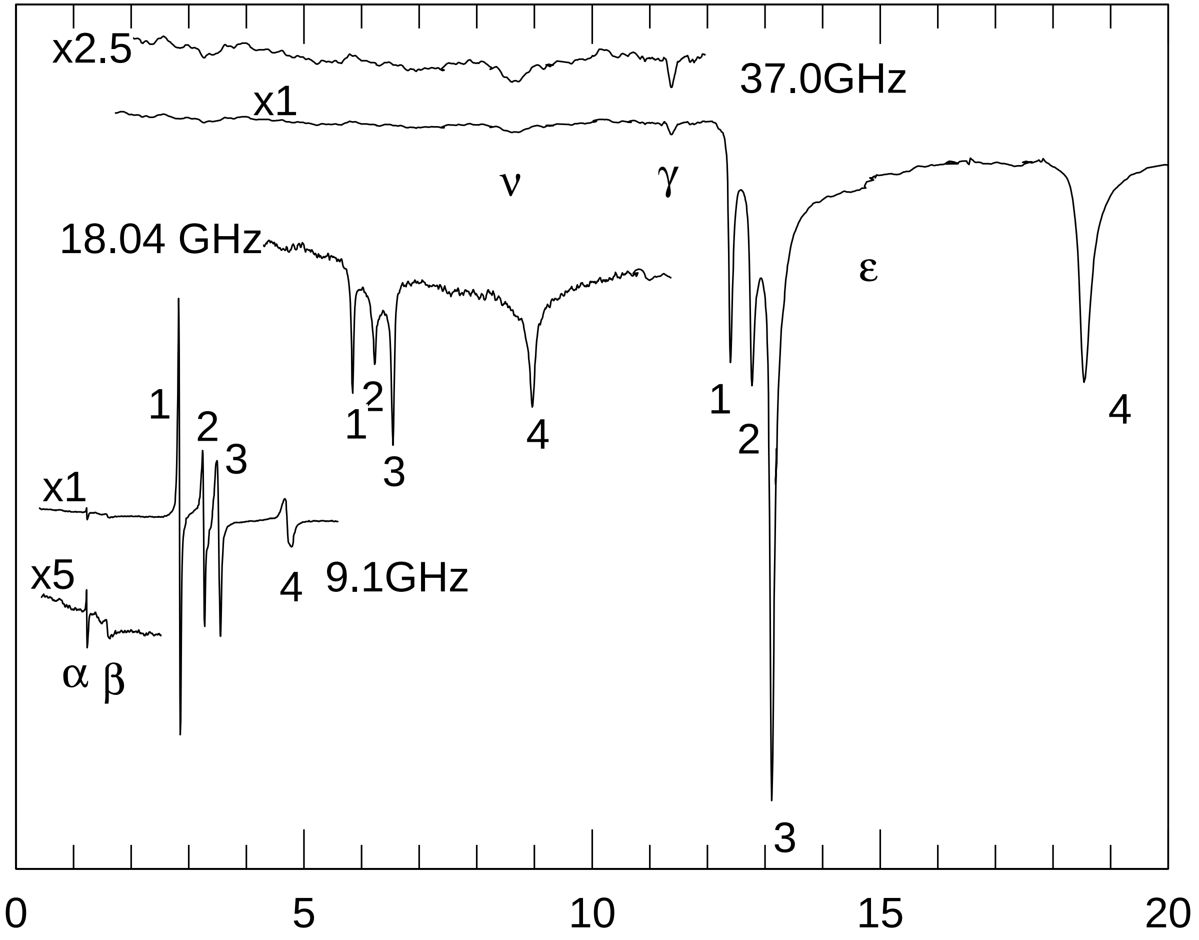

x2.5
37.0GHz
x1
ν
γ
18.04 GHz
ε
1
2
1
2
3
4
1
2
3
4
x1
x5
4
9.1GHz
α
β
3
0
5
10
15
20
H,KOe

Fig.2

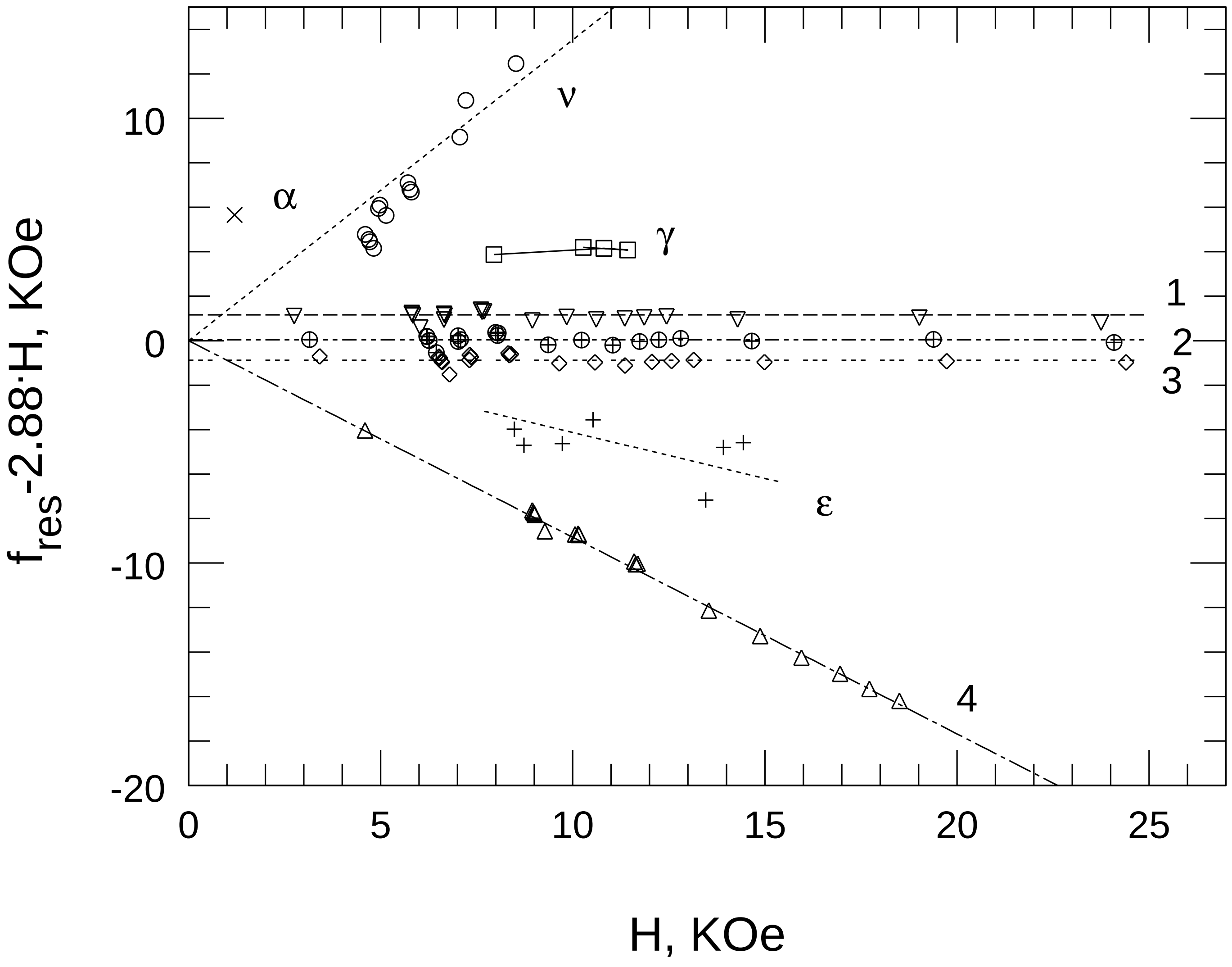

Fig.3

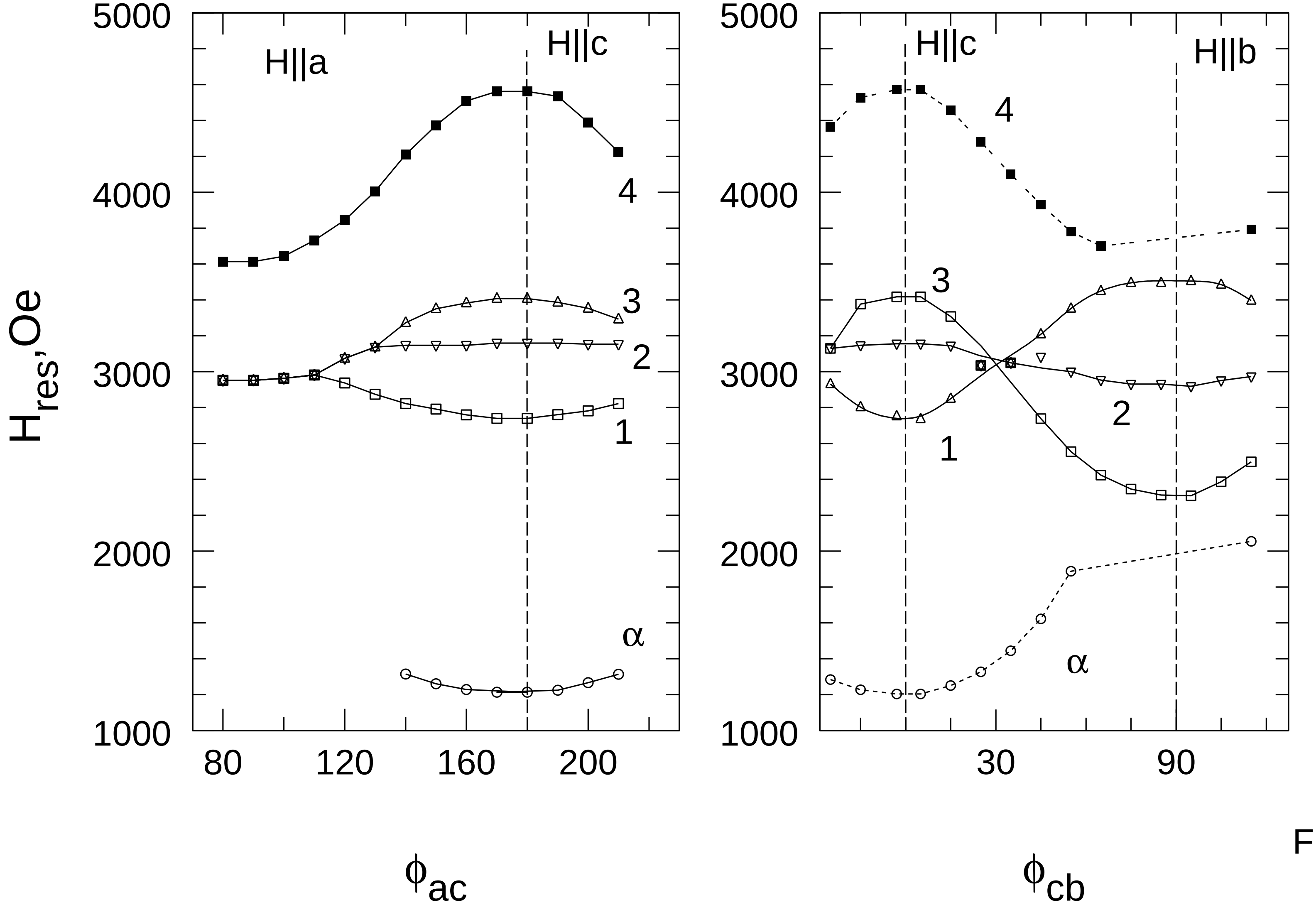
H_{res},Oe
5000
4000
3000
2000
1000
H||a
H||c
4
3
2
1
α
80
120
160
200
ϕ_{ac}
5000
4000
3000
2000
1000
H||c
H||b
4
3
2
1
α
30
90
ϕ_{cb}

Fig.4

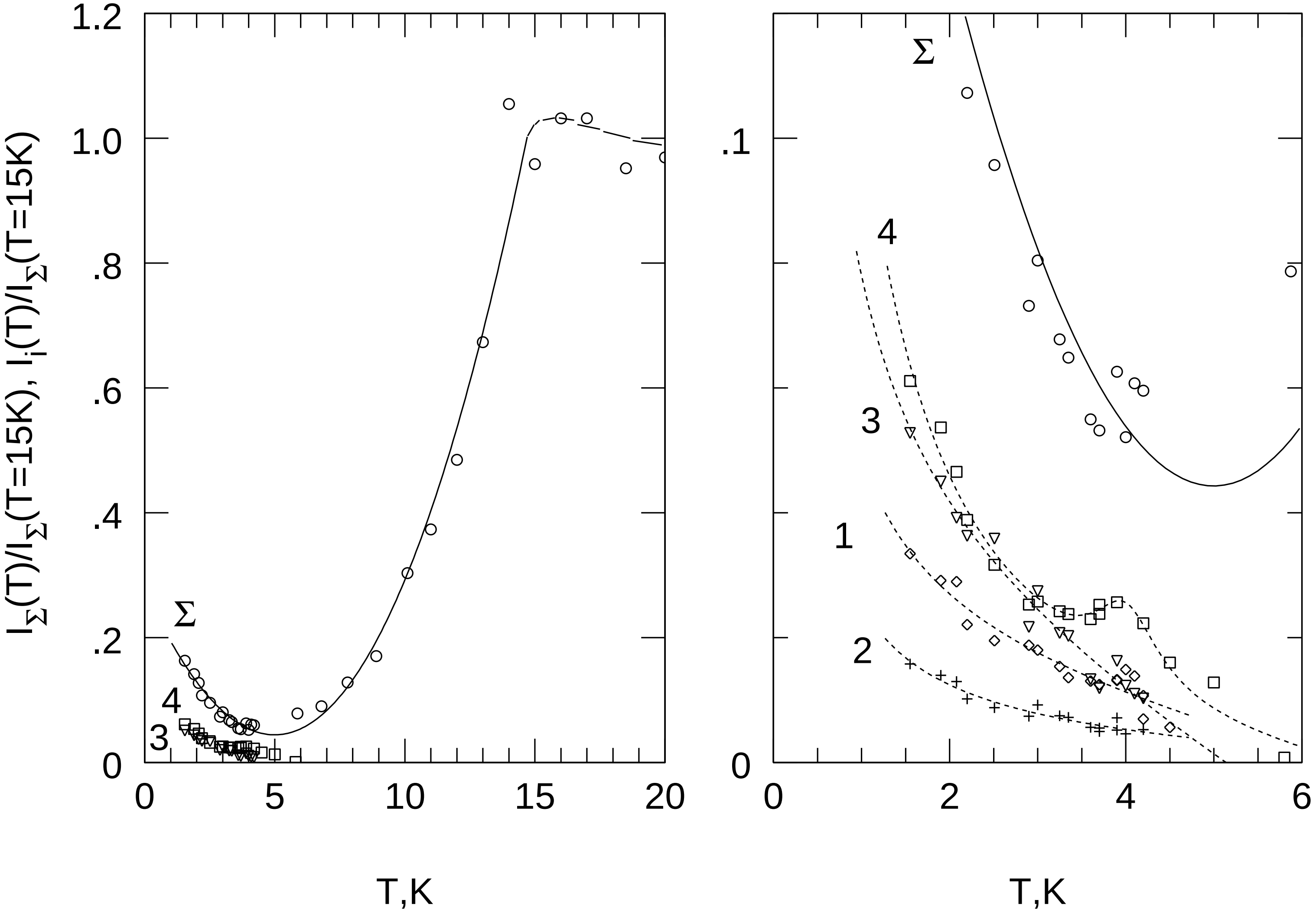

$I_\Sigma(T)/I_\Sigma(T=15K)$, $I_i(T)/I_\Sigma(T=15K)$
1.2
1.0
.8
.6
.4
.2
0
0
5
10
15
20
T,K
Σ
4
3
.1
0
0
2
4
6
T,K
Σ
4
3
1
2

Fig.5

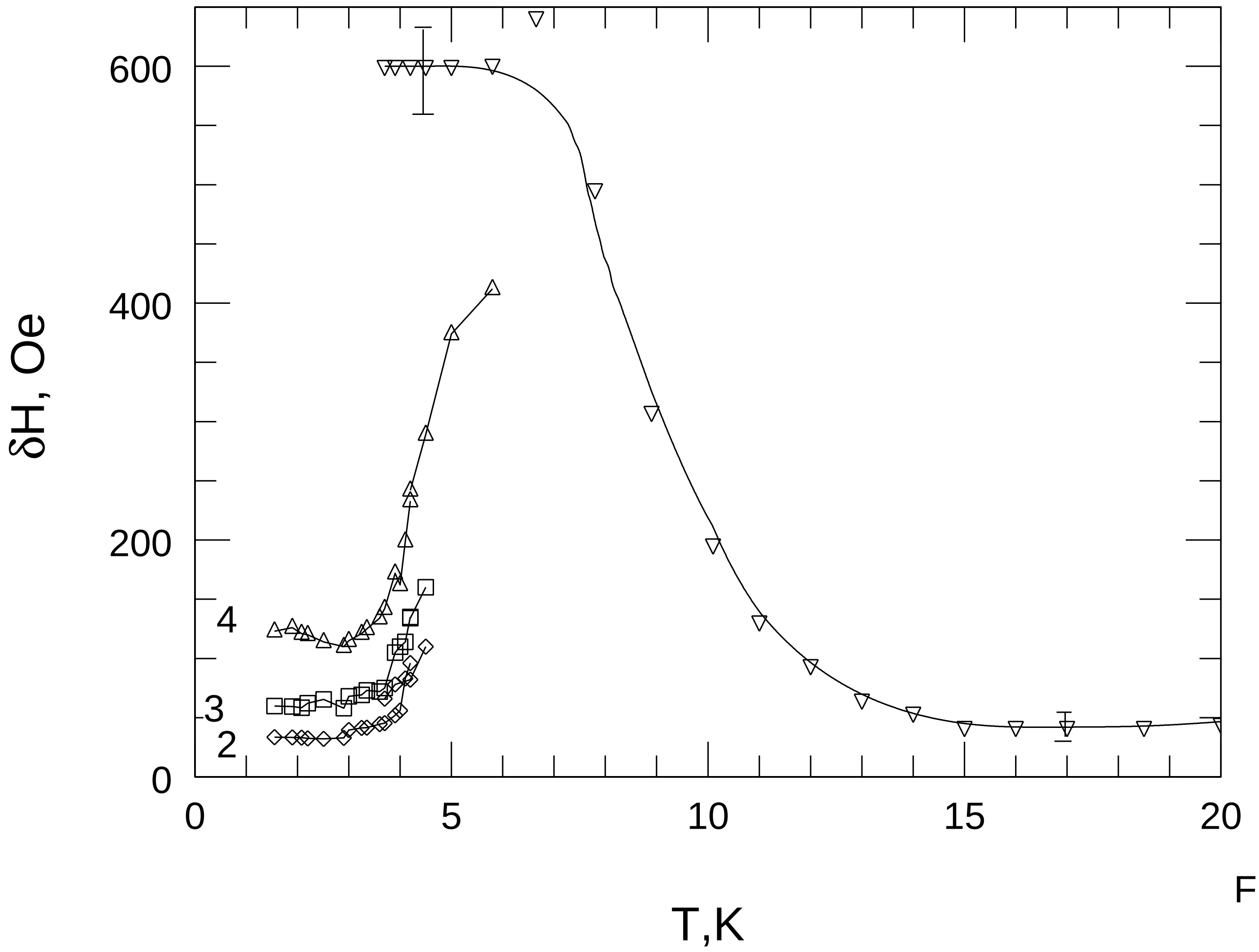

Fig.6

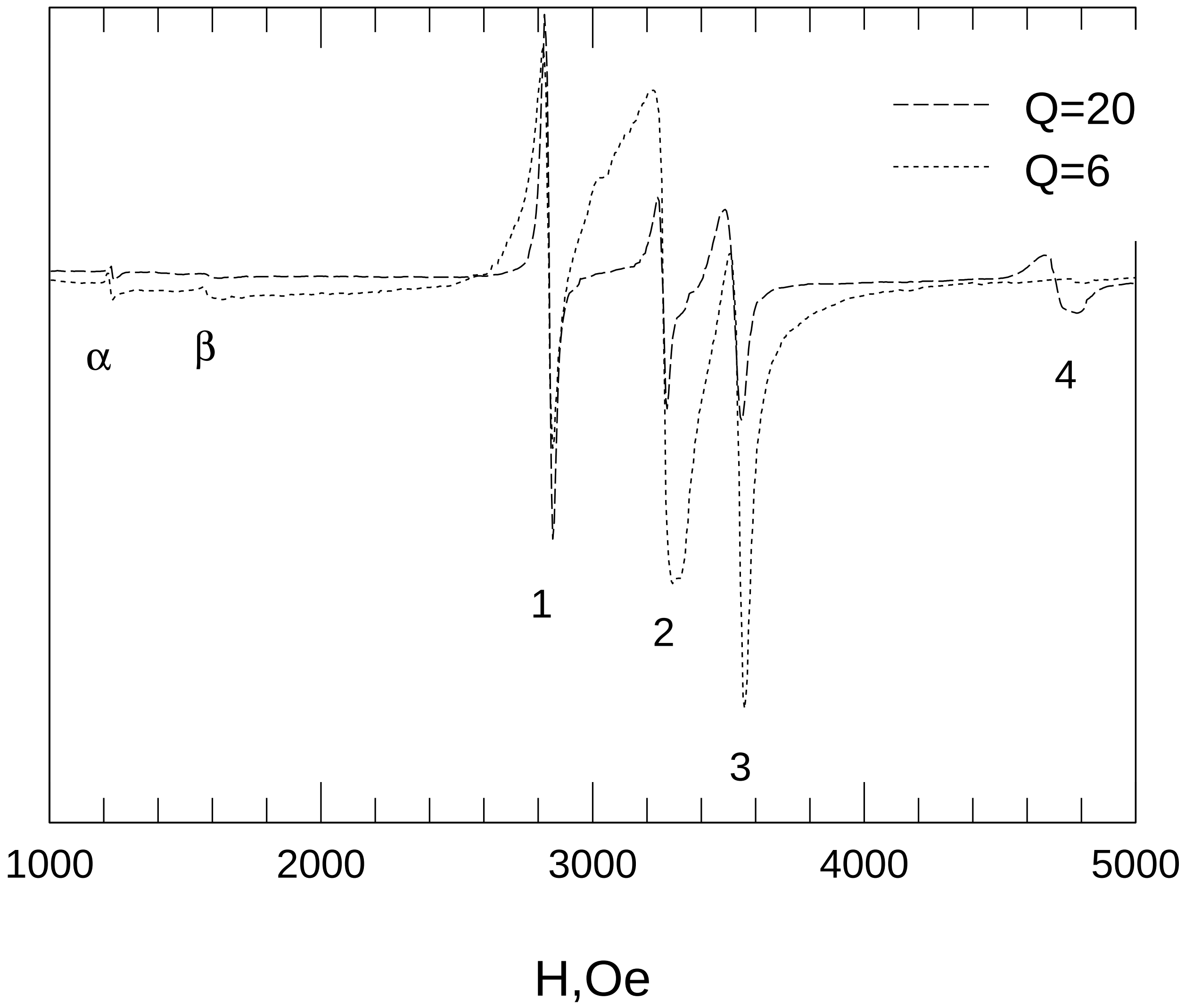

Fig.7

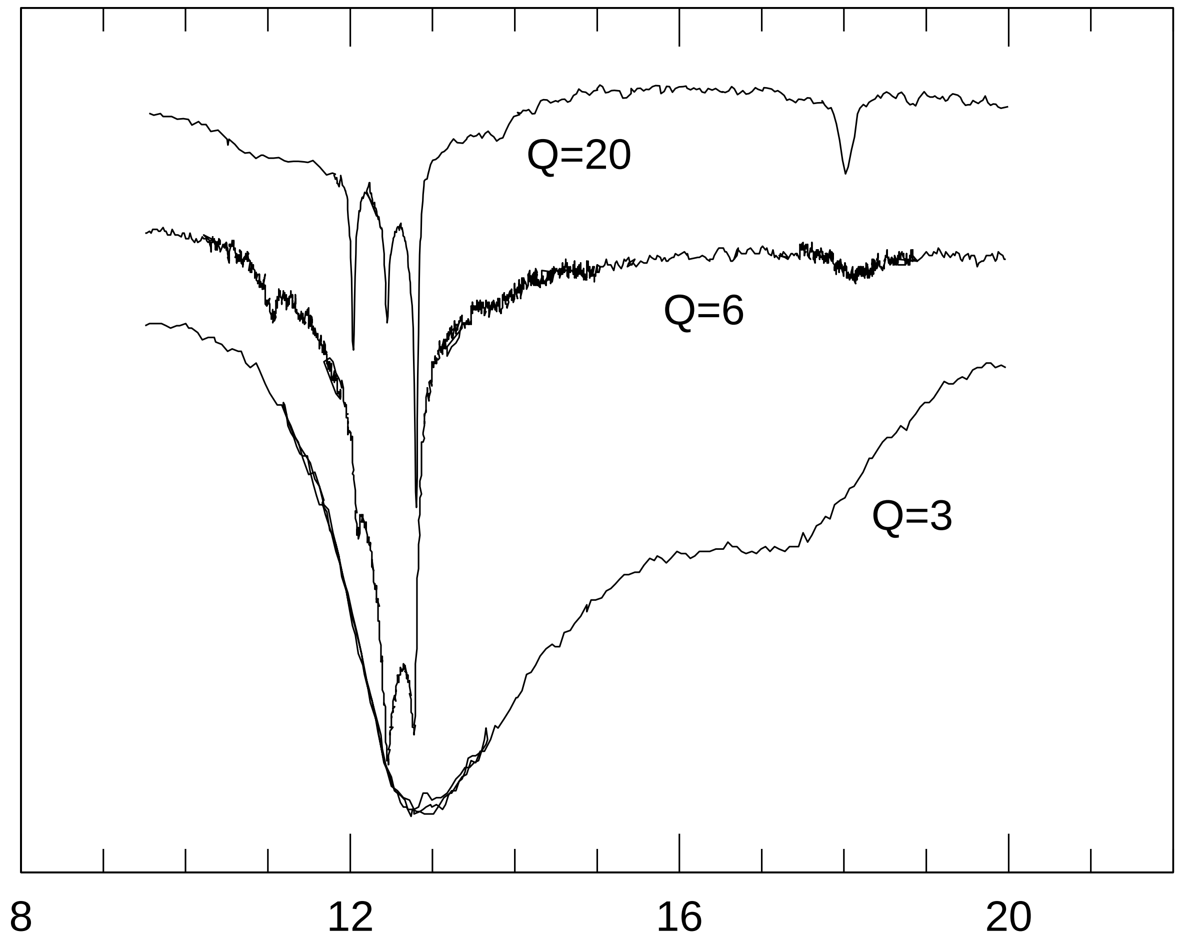

Fig.8

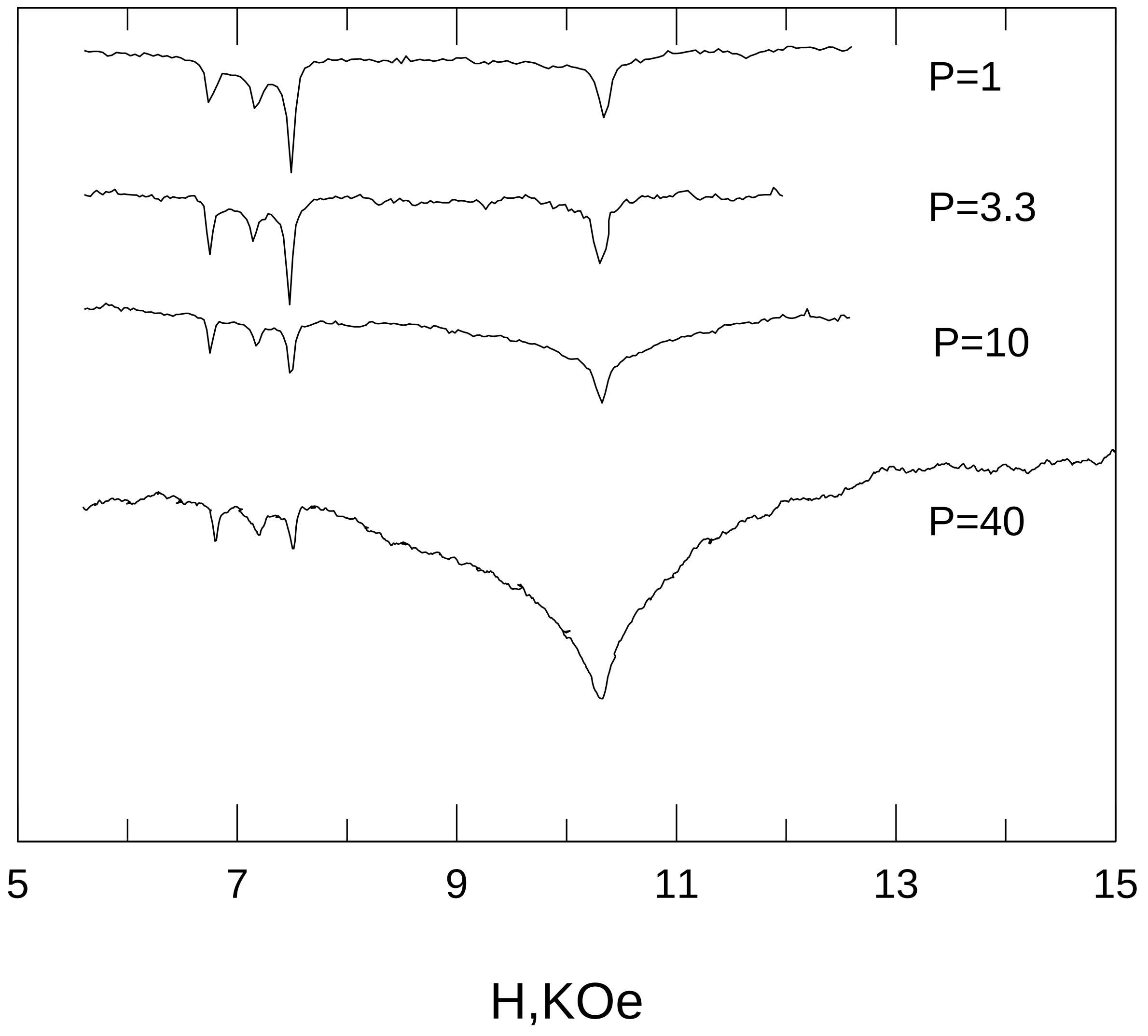

Fig.9

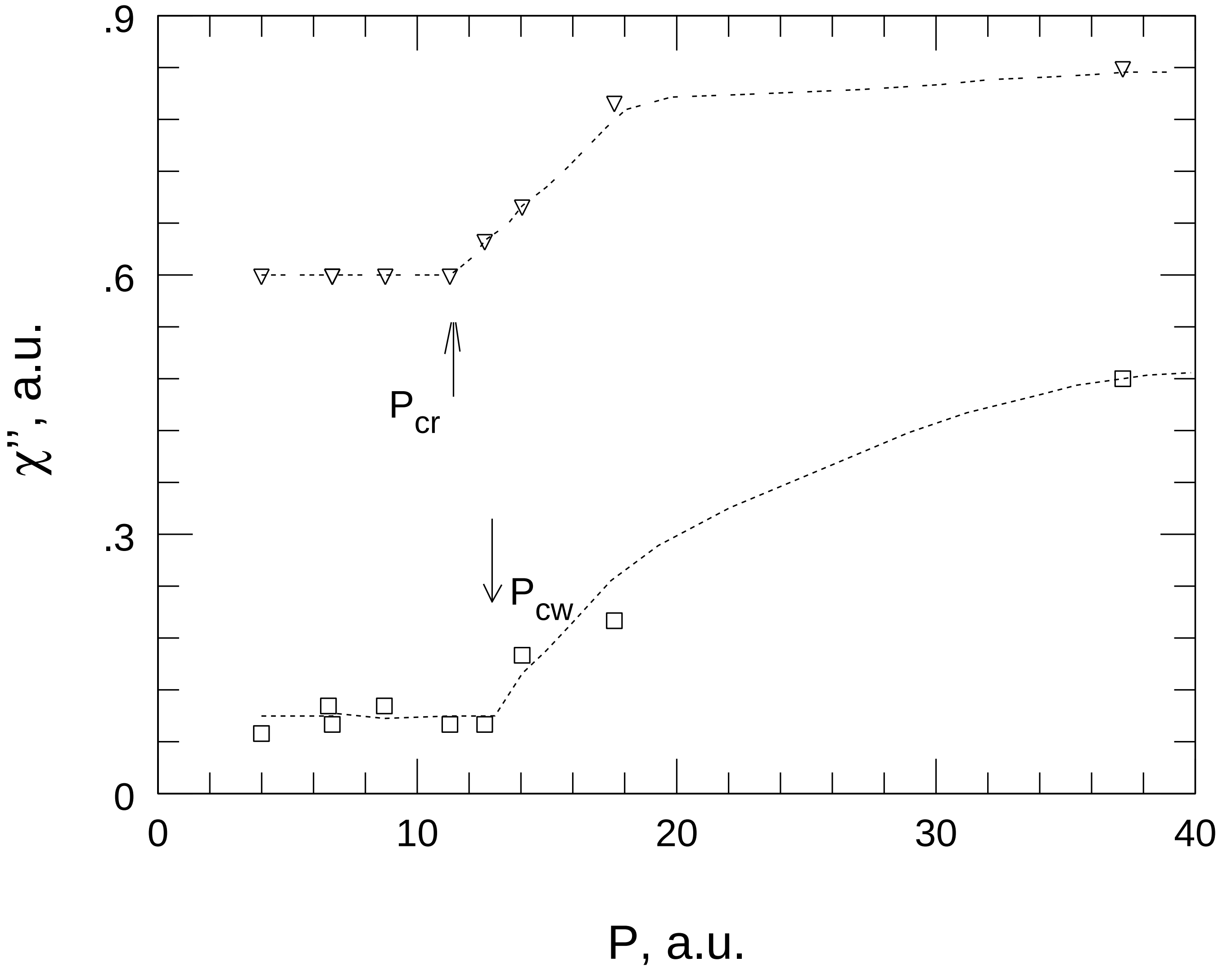

Fig.10

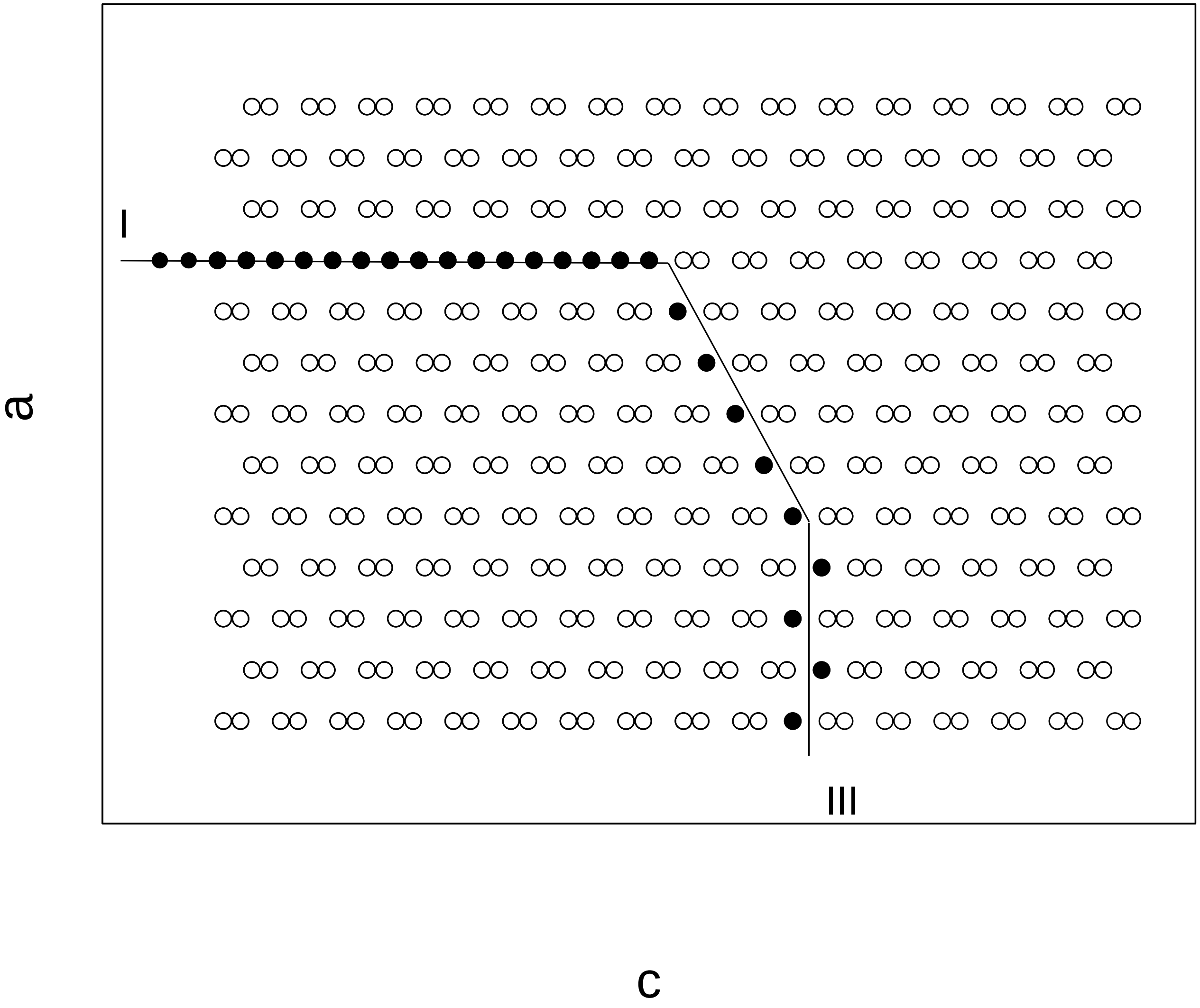

Fig.11

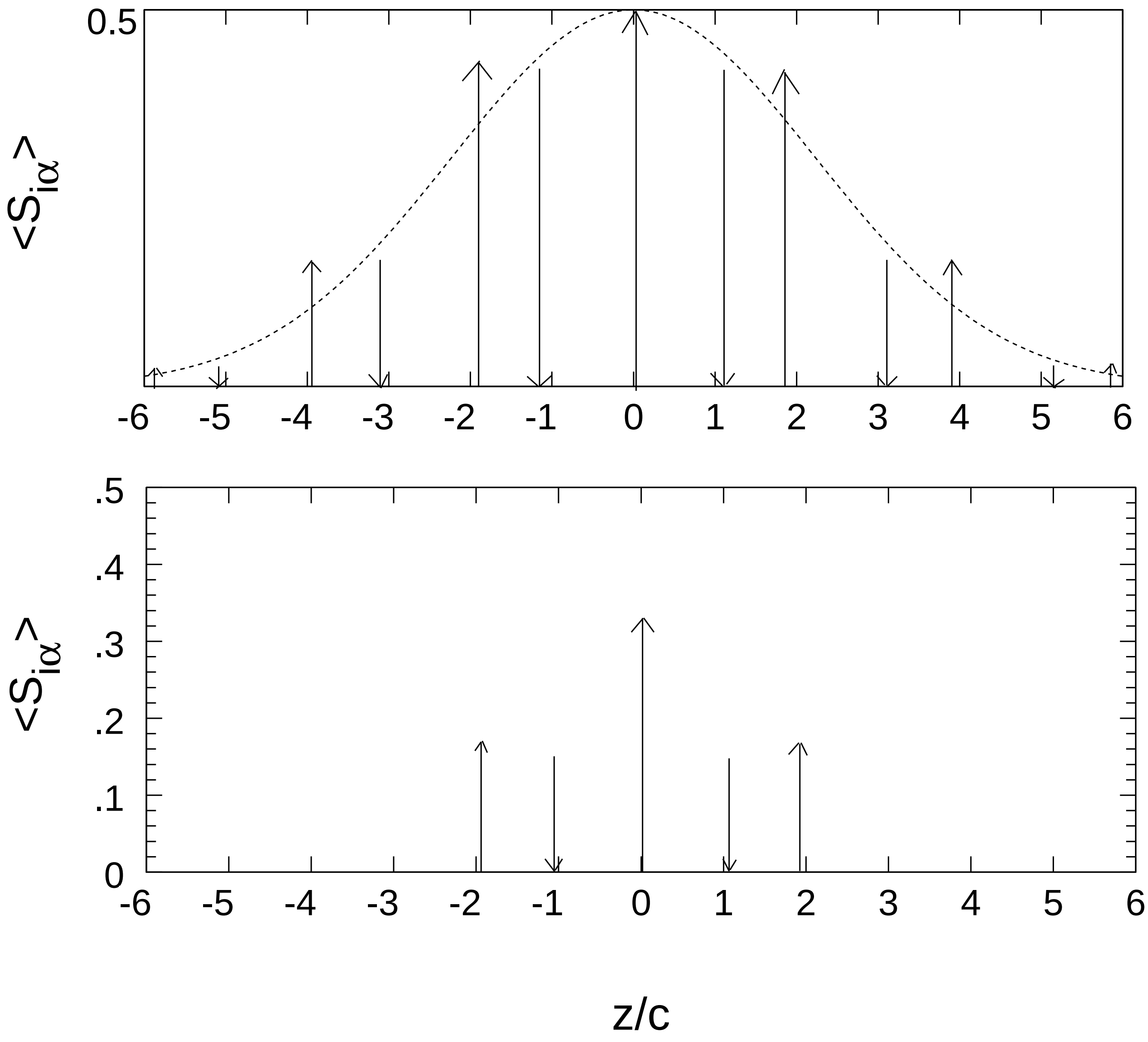

Fig.12